frontiers | Frontiers in Energy Research

TYPE Original Research
PUBLISHED 25 September 2024
DOI 10.3389/fenrg.2024.1485135

OPEN ACCESS

EDITED BY
Minghao Wang,
University of Macau, China

REVIEWED BY
Xu Xu,
Xi'an Jiaotong-Liverpool University, China
Jiapeng Li,
Xi'an Jiaotong University, China

*CORRESPONDENCE
Mengwei Zhang,
2464152664@hnu.edu.cn

RECEIVED 23 August 2024
ACCEPTED 13 September 2024
PUBLISHED 25 September 2024

CITATION
Sun P, Zhang M, Liu H, Dai Y and Rao Q (2024) Coordinated scheduling of 5G base station energy storage for voltage regulation in distribution networks.
Front. Energy Res. 12:1485135.
doi: 10.3389/fenrg.2024.1485135

Coordinated scheduling of 5G base station energy storage for voltage regulation in distribution networks

Peng Sun, Mengwei Zhang*, Hengxi Liu, Yimin Dai and Qian Rao

College of Electrical and Information Engineering, Hunan University, Changsha, China

With the rapid development of 5G base station construction, significant energy storage is installed to ensure stable communication. However, these storage resources often remain idle, leading to inefficiency. To enhance the utilization of base station energy storage (BSES), this paper proposes a co-regulation method for distribution network (DN) voltage control, enabling BSES participation in grid interactions. In this paper, firstly, an energy consumption prediction model based on long and short-term memory neural network (LSTM) is established to accurately predict the daily load changes of base stations. Secondly, a BSES aggregation model is constructed by using the power feasible domain maximal inner approximation method and Minkowski summation to evaluate the charging and discharging potential and adjustable capacity of BSES clusters. Subsequently, a BSES demand assessment and optimal scheduling model for low voltage regulation in DN is developed. This model optimizes the charging and discharging strategies of BSES to alleviate low voltage problems in DN. Finally, the simulation results effectively verify the feasibility of the proposed optimal scheduling method of BSES for voltage regulation in DN.

KEYWORDS

5G base station energy storage, aggregation, distribution network, voltage regulation, optimal scheduling

1 Introduction

In recent years, advancements in new energy technologies have progressed rapidly, and the proportion of new energy sources such as wind energy and solar energy has been increasing. The landscape of large-scale new energy consumption remains unclear, necessitating urgent adjustments in flexible resource allocation. As the best flexible resource, energy storage can control the input and output of power and energy at different time scales, thereby improving the stability and operation characteristics of high-proportion new energy power systems, promoting flexible dispatching of power grids, and solving the adverse effects of large-scale grid-connected clean energy. However, its widespread adoption is impeded by high costs. Meanwhile, China has clearly proposed to speed up the development of new infrastructure. Operators of 5G base stations have invested in constructing numerous communication facilities and configured extensive energy storage batteries to ensure the stability and reliability of communication. However, the growing strength and stability of the distribution system have significantly enhanced the energy supply reliability of 5G base stations, making the redundant 5G BSES devices idle for a long time. Therefore, considering the unique backup

power supply requirements of energy storage resources at communication base stations, it is urgent to investigate the influence of the communication load characteristics on the backup power demand and deeply explore the schedulable potential of the backup energy storage. This will enable the efficient utilization of idle resources at 5G base stations in the collaborative interaction of the power system, fostering mutual benefit and win-win between the power grid and the communication operators.

The research on 5G base station load forecasting technology can provide base station operators with a reasonable arrangement of energy supply guidance, and realize the energy saving and emission reduction of 5G base stations. Currently, the research primarily focuses on statistical learning methods and machine learning techniques (Shang et al., 2022). In (Morosi et al., 2013), the exponential smoothing technique is used to predict the traffic in all coverage areas of the base station. In (Pan et al., 2015), a Block Regression (BR) model for base station traffic prediction considering the time correlation of base station load is proposed. Although the proposed model boasts low complexity and the mathematical formula is clear and easy to understand, it suffers from poor scalability as it constructs only a single model for all base stations. Moreover, the prediction results using these statistical learning models are not satisfactory when dealing with long-term problems, especially when predicting violently fluctuating base station network traffic data (Cheng et al., 2023). For the machine learning load forecasting model, a neural network load forecasting training method based on the maximum correntropy criterion (NTPMCC) is proposed in (Qu et al., 2013). This method takes into account the nonlinear characteristics of network load, but the overall improvement in prediction accuracy is moderate. Reference (Qu et al., 2019) introduces a base station load forecasting model that leverages spatio-temporal characteristics. To achieve this, a clustering algorithm based on artificial neural networks is employed to establish specific models for various types of base stations. Additionally, in reference (Stolojescu-Crisan, 2012), the Stationary Wavelet Transform (SWT) method is introduced during the data preprocessing stage. This method is combined with the Auto-Regressive Integrated Moving Average (ARIMA) model and Artificial Neural Networks (ANNs) to accomplish the load forecasting tasks. While the above-mentioned base station load forecasting method cannot shield the interference caused by the drastic fluctuation of 5G base station load data, which leads to a large static error in the prediction results, so there is an urgent need to study a more efficient and applicable base station load prediction method to effectively improve the base station load prediction accuracy.

Addressing the efficient utilization of flexible resources in 5G base stations, literature (Ye, 2021; Yin et al., 2022) proposes installing photovoltaic systems to enhance energy storage capabilities. However, for the existing 5G base stations that have been completed, the measure of reinstalling photovoltaic devices is difficult to implement. Several scholars have proposed a dynamic clustering method of energy storage utilizing virtual power plant technology to address the challenge that the energy storage of communication base stations with a large number and wide distribution is difficult to schedule (Suo et al., 2022; Yang et al., 2020). Nevertheless, the energy storage model is too simplified, and the spatial and temporal differences between BSES are ignored in order to improve the solution efficiency. Other studies have deeply explored the adjustable capacity of energy storage, and proposed energy storage resource aggregation optimization methods (Yang et al., 2023; Yu et al., 2023). Reference (Sajjad et al., 2016) pointed out that the idea of describing the feasible region of energy storage resource cluster operation can be divided into two kinds: top-down and bottom-up. Among them, top-down refers to the direct construction of the feasible region of cluster operation through data analysis and probabilistic modeling. From bottom to top, it refers to describing the feasible domain of a single resource first, and then aggregating multiple independent operating domains into a unified whole. Following a top-down approach, reference (Sajjad et al., 2016) estimates the flexibility level according to the probability of changing the collective behavior of aggregated users. Reference (Ma et al., 2013) developed a flexibility standard based on reinforcement learning methods to distinguish different load types, thereby assessing the total adjustment potential of resources. The current mainstream research tends to be bottom-up, considering the shortcomings of complexity, uncertainty, high computational cost and poor interpretability in constructing feasible regions directly through data analysis and probabilistic modeling. Following a bottom-up approach, reference (Müller et al., 2019) pointed out that the flexibility of each resource is mathematically regarded as a feasible region bounded by polytope, and the essence of the flexibility aggregation problem is the Minkowski sum of polytope provided by all flexible resources. However, the above method is not feasible in practical solution. As the dimension of the polyhedron increases, both the number of vertices and the permutations and combinations grow exponentially. This results in a phenomenon known as dimension explosion (Barot and Taylor, 2017; Althoff et al., 2010), significantly escalating the computational complexity of Minkowski summation. In (Müller et al., 2019), the zonotope set was proposed to aggregate distributed resource flexibility. The internal approximation method of the power feasible region ensures the feasibility of the model solution, but it also entails varying degrees of flexibility loss. The above research focuses on aggregating multiple flexible resources in the power system, but does not systematically investigate aggregation methods as backup resources for BSES. Therefore, it is necessary to thoroughly consider the characteristics of the standby power supply of the BSES resources, conduct in-depth research on its dynamic aggregation method, and quantitatively evaluate the power adjustment ability of the BSES cluster.

Research on 5G BSES in the power system focuses on integrating with the operation and dispatching of the DN (Li et al., 2022). The primary objective is to support the DN in integrating new energy consumption (Liang et al., 2023), peak shaving, valley filling (Yang et al., 2023), and optimizing economic dispatching (Chai et al., 2014). In (Jia et al., 2023), research focuses on mobile energy storage technology aimed at enhancing the consumption of distributed energy within station areas, which improves the consumption rate of new energy and ensures the stable and reliable operation of the DN in the station area. Reference (Zhang et al., 2023) proposed a model to optimize the energy storage configuration of 5G base stations. The objective is to alleviate the pressure of peak load on the power grid by minimizing the total investment over the battery system's entire lifecycle. Reference (Han et al., 2021) proposed a Stackelberg game collaborative optimization method for DN and 5G mobile network based on demand response. The DN operator (DNO) acts as the leader, selecting an optimal interactive electricity price to reduce peak-valley differences in net load. The mobile network operator (MNO), as a follower, adjusts its energy costs by responding to the electricity price set by the DNO. In (Zhou and Xu, 2021), the mobile BSES system is

used to provide local reactive power support. A day-ahead reactive power scheduling model is proposed, considering the system and the conventional reactive power compensation device, aimed at minimizing the node voltage deviation in the active DN. The above research works have established methods for BSES to participate in DN optimization and dispatch from different perspectives, but there is a lack of research related to making full use of BSES resources to participate in voltage regulation of DNs.

In summary, the existing research on 5G BSES lacks a BSES co-regulation method based on aggregation technology for voltage regulation of DNs. Therefore, in order to fill the above research gaps, this paper firstly proposes a BSES aggregation model taking into account the base station energy consumption prediction, and then proposes a BSES co-regulation method for the voltage regulation of base stations in distribution grids, which makes full use of the large amount of idle energy storage resources in 5G base stations and realizes the mutual benefits of telecommunication operators and power grids. The main contributions of this paper are as follows.

- The specific composition of 5G base station energy consumption is analysed, and a 5G base station energy consumption prediction model based on long short-term memory (LSTM) is constructed.
- Considering the power supply characteristics of BSES backup supply, we constructed a BSES aggregation model taking into account the energy consumption prediction of 5G base stations, and quantitatively evaluated the maximum adjustable capacity and charging/discharging potential of BSES.
- A BSES co-regulation method based on BSES aggregation technology for voltage regulation of DNs is proposed to quantitatively assess the minimum energy storage regulation capacity required for voltage regulation of DNs and optimize the charging and discharging strategy of each BSES based on the balanced charge state scheduling method of energy storage.

The rest of this paper is organized as follows: In Section 2, it proposes a method for predicting 5G base station energy consumption using LSTM and constructs a BSES aggregation model considering this prediction. In Section 3, it proposes a coordinated control method of BSES for low voltage governance of DN based on BSES aggregation technology. In Section 4, simulations are performed on a real distribution network test system. The conclusion is put forward in Section 5.

2 BSES aggregation method considering energy consumption prediction

2.1 5G base station energy consumption analysis and prediction model

2.1.1 5G base station energy consumption model

To meet the communication requirements of large capacity and low delay, the commissioning of new equipment has significantly improved the performance of 5G base stations compared with the previous generation base stations. At the same time, the new equipment has altered the power load characteristics of base stations. In the 5G technology framework, the 5G base station comprises macro and micro variants. The micro base station serves indoor blind spots with minimal power consumption. The macro base station exhibits greater potential for demand response. This section primarily analyzes the current mainstream commercial 5G macro base stations.

The load of a 5G base station primarily consists of communication equipment and auxiliary components. The communication equipment mainly includes Active Antenna Unit (AAU) and Base Band Unit (BBU). AAU is a combination of radio frequency unit and antenna array of 5G base station. Its main functions include converting baseband digital signal into analog signal, modulating it into high frequency radio frequency signal, and then amplifying it to enough power to be transmitted through the antenna. AAU is the most energy-consuming equipment in 5G base stations, accounting for up to 90% of their total energy consumption. Auxiliary equipment includes power supply equipment, monitoring and lighting equipment. The power supply equipment manages the distribution and conversion of electrical energy among equipment within the 5G base station. During main power failures, the energy storage device provides emergency power for the communication equipment.

A set of 5G base station main communication equipment is generally composed of a baseband BBU unit and multiple RF AAU units. Equation 1 serves as the base station load model:

$$P_{BS} = P_{\text{main}} + P_{\text{static}} \tag{1}$$

where P_{BS} is base station load; P_{main} is the base station main equipment load power and $P_{\text{main}} = P_{\text{BBU}} + n \cdot P_{\text{AAU}}$, P_{BBU} is the baseband unit power, n is the number of active antenna elements, P_{AAU} is the active antenna unit power and its size is mainly related to the base station communication load; P_{static} is the base station auxiliary equipment load power, including the base station environment equipment, transmission equipment and monitoring equipment load power, and the power remains constant.

The load change of base station mainly depends on the communication behavior of users, exhibiting significant time correlation and random fluctuations. As a special deep recurrent neural network, the LSTM network can basically smooth the interference caused by fluctuation to the training model, making it suitable for base station energy consumption prediction with large fluctuations in time series data.

2.1.2 LSTM-based energy consumption prediction model for 5G base stations

The LSTM model is an advanced extension of the Recurrent Neural Network (RNN) model, specifically designed to handle sequence data. It addresses the long-term dependency problem, enabling it to better capture long-term dependencies in sequence data. This allows the model to effectively learn patterns and features in temporal data.

According to the energy consumption characteristics of the base station, a 5G base station energy consumption prediction model based on the LSTM network is constructed to provide data support for the subsequent BSES aggregation and collaborative scheduling. The prediction flow chart is shown in Figure 1, and the specific prediction process is as follows.

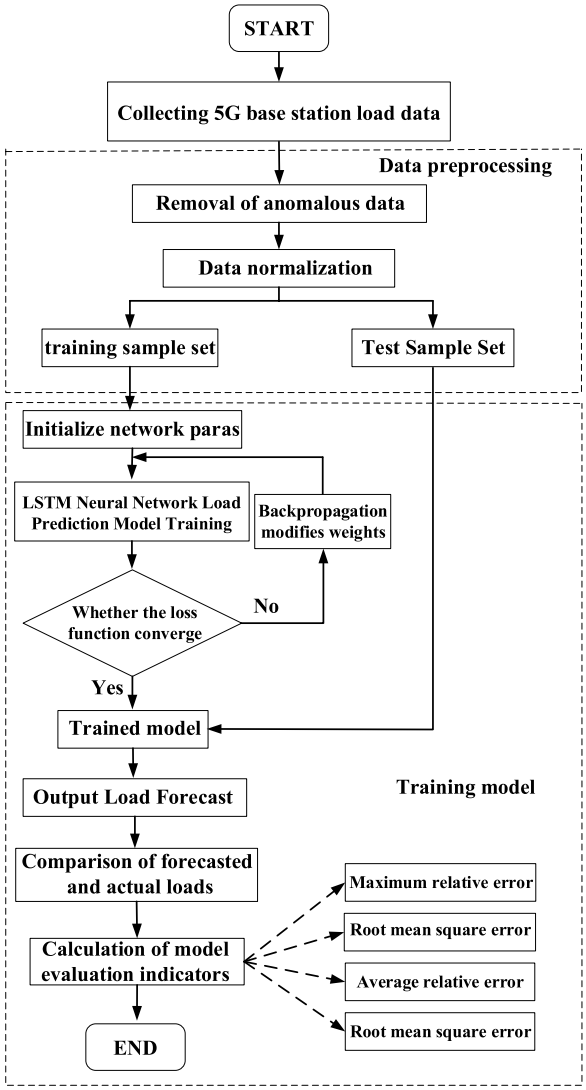

FIGURE 1
Flowchart of 5G base station load prediction based on LSTM.

Step (1) The data is collected and preprocessed. After deleting the abnormal data, the data is normalized according to Equation 2. Then, the processed data set is divided into training set and test set according to a certain proportion.

$$P_{bs} = \frac{P - P_{min}}{P_{max} - P_{min}} \tag{2}$$

where P_{bs} is the normalized historical input data; P is the historical input data before normalization; P_{min} is the minimum value of the historical input data before normalization; P_{max} is the maximum value of the historical input data before normalization.

Step (2) The LSTM model is created and the training set sample data is imported into the LSTM load forecasting model for training. The specific LSTM model principle can be referenced in (Fu, 2020).

Step (3) The test set sample data is imported into the trained model for 5G base station load forecasting, and compared with the actual 5G base station load to calculate the evaluation index of the model. The root mean square error e_{RTS}, average relative error e_{AR}, maximum relative error e_{MR} and relative error e_R are used as the evaluation indexes of prediction effect. The calculation formula is as Equations 3–6:

$$e_{RTS} = \sqrt{\frac{1}{n}\sum_{i=1}^{n}(y_i - \hat{y}_i)^2} \tag{3}$$

$$e_{AR} = \frac{1}{n}\sum_{i=1}^{n}\left|\frac{y_i - \hat{y}_i}{y_i}\right| \tag{4}$$

$$e_{MR} = \max\left(\left|\frac{y_i - \hat{y}_i}{y_i}\right|\right) \tag{5}$$

$$e_R = \left|\frac{y_i - \hat{y}_i}{y_i}\right| \tag{6}$$

where y_i is the actual load value; $\hat{y}_i$ is the load prediction value; n is the number of data sets.

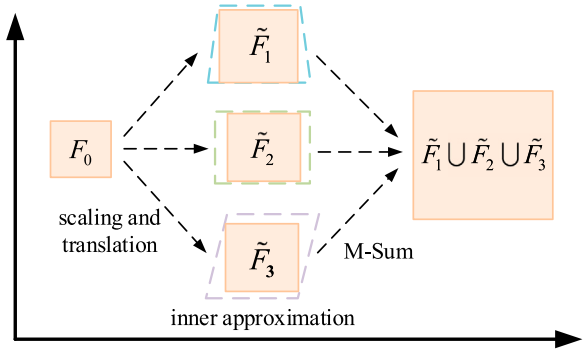

FIGURE 2
The principle of the maximum inner approximation method in the feasible domain of aggregation power.

2.2 BSES aggregation method

2.2.1 Operational model of individual BSES

The feasible domain of a single BSES power can be described as:

$$F_j = \left\{ \mathbf{p}_j^{ES} \in \mathbb{R}^T \left| \begin{array}{c} E_{j,t}^{ES} = \delta_j E_{j,t-1}^{ES} + p_{j,t}^{ES}\Delta t, \forall t \in \tau \\ -p_{j,t}^{ES,-} \le p_{j,t}^{ES} \le p_{j,t}^{ES,+}, \forall t \in \tau \\ E_{j,t}^{ES,-} \le E_{j,t}^{ES} \le E_{j,t}^{ES,+}, \forall t \in \tau \end{array} \right. \right\} \tag{7}$$

where $\mathbf{p}_j^{ES}$ is the output power of the BSES j at each moment in the time period T, while $\mathbf{p}_j^{ES} = [p_{j,1}^{ES}, p_{j,2}^{ES}, \cdots, p_{j,T}^{ES}]$; $E_{j,t}^{ES}$ is the battery residual energy state of the BSES j at time t; δ_j is the self-discharge efficiency of the BSES j; $p_{j,t}^{ES}$ is the input power of the BSES j at time t, $p_{j,t}^{ES} > 0$ indicates charging, $p_{j,t}^{ES} < 0$ indicates discharging,; is charging/discharging intervals for BSES j; $\tau = \{1, 2, \cdots, T\}$, denotes a moment in time T; $p_{j,t}^{ES,-}$ is the maximum discharge power of the BSES j; $p_{j,t}^{ES,+}$ is the maximum charge power of the BSES j; $E_{j,t}^{ES,-}$ is the value of the minimum energy state allowed for the BSES j at time t, with respect to the load size and minimum supply time at time t, $E_{j,t}^{ES,-} = t_{\min}^{d} P_t^d$, P_t^d is the predicted power of the base station energy consumption at time t, is the minimum power supply

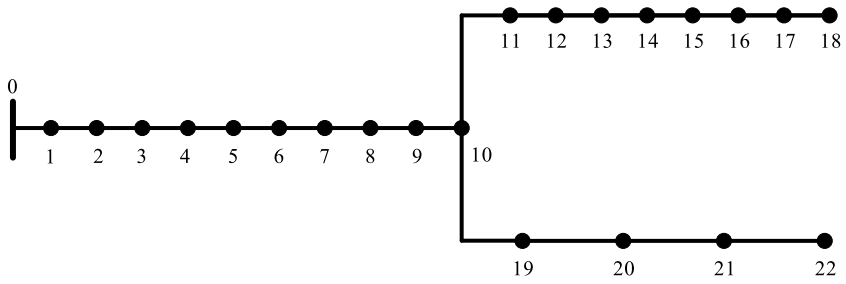

FIGURE 3
Topology of 22-node distribution network system.

TABLE 1 Line parameters.

Line	Length (km)	Resistance (Ω/km)	Reactance (Ω/km)	Current capacity (A)
0–10	13.173	0.13	0.358	503
10–16	4.176	0.91	0.38	90
16–18	1.364	0.91	0.38	90
10–20	4.266	0.91	0.38	90
20–22	4.635	0.91	0.38	90

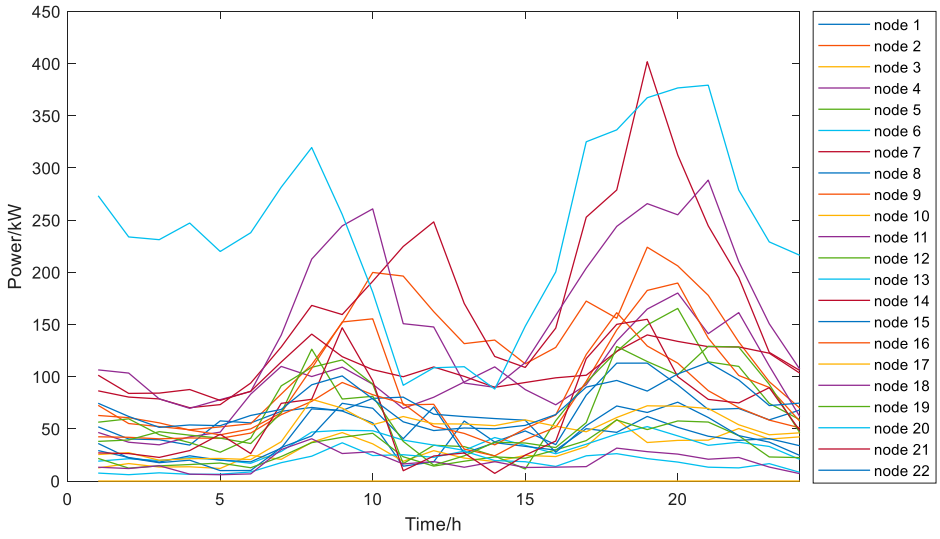

FIGURE 4
Load curve of each node.

time of the base station load, and the general minimum power supply time is 3 h; and $E_{j,t}^{ES,+}$ is the maximum energy state value of the BSES j allowed at time t.

To facilitate the derivation of the subsequent equations, Equation 7 can be written in the following compact form, as illustrated in Equation 8.

$$F_j = \left\{ \mathbf{p}_j^{ES} \in \mathbb{R}^T \middle| \mathbf{M}_j \mathbf{p}_j^{ES} \le \mathbf{N}_j \right\} \tag{8}$$

where $\mathbf{M}_j$, $\mathbf{N}_j$ are expressed as Equations 9, 10, respectively:

$$\mathbf{M}_j = \left(diag(\mathbf{I}); diag(-\mathbf{I}); \mathbf{A}_j^{-1}\mathbf{B}_j; -\mathbf{A}_j^{-1}\mathbf{B}_j \right) \tag{9}$$

$$\mathbf{N}_j = \left(\mathbf{p}_j^{ES,+}; \mathbf{p}_j^{ES,-}; \mathbf{E}_j^{ES,+} - \mathbf{A}_j^{-1}\mathbf{C}_j; -\mathbf{E}_j^{ES,-} + \mathbf{A}_j^{-1}\mathbf{C}_j \right) \tag{10}$$

where $\mathbf{I} = [1, 1, \cdots, 1]^T \in \mathbb{R}^{T\times 1}$, where $\mathbf{p}_j^{ES,+}$, $\mathbf{p}_j^{ES,-}$, $\mathbf{E}_j^{ES,+}$, $\mathbf{E}_j^{ES,-} \in \mathbb{R}^{T\times 1}$, represent maximum charging power vector, the maximum discharging vector, the maximum energy state vector and the minimum energy state vector of the BSES j in T period, respectively. $\mathbf{A}_j$, $\mathbf{B}_j$, $\mathbf{C}_j$ are expressed as Equations 11-13, respectively:

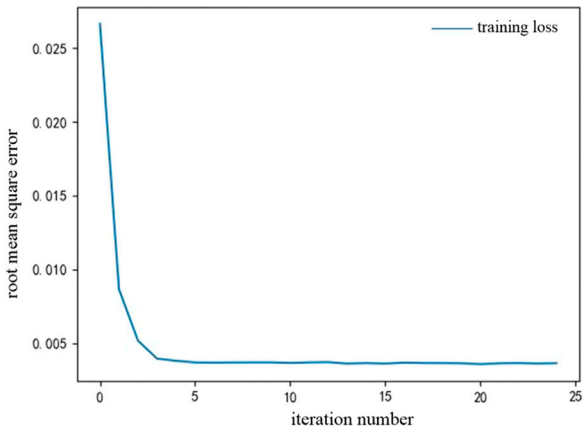

FIGURE 5
Convergence of training set error for 5G base station energy consumption prediction.

$$\mathbf{A}_j = \begin{bmatrix} 1 & 0 & 0 & \cdots & 0 \\ -\delta_j & 1 & 0 & \cdots & 0 \\ 0 & -\delta_j & 1 & \cdots & 0 \\ \vdots & \vdots & \vdots & \ddots & \vdots \\ 0 & 0 & 0 & \cdots & 1 \end{bmatrix} \tag{11}$$

$$\mathbf{B}_j = diag(\mathbf{I})\Delta t \tag{12}$$

$$\mathbf{C}_j = \left[\delta_j E_{j,0}^{ES}, 0, 0\cdots, 0\right]^T \tag{13}$$

where $\mathbf{A}_j, \mathbf{B}_j \in \mathbb{R}^{T\times T}$, $\mathbf{C}_j \in \mathbb{R}^{T\times 1}$. δ_j is the self-discharge efficiency of the BSES j. $E_{j,0}^{ES}$ is the initial capacity state of energy storage.

2.2.2 BSES aggregation model

To reduce decision-making complexity at the distribution network operator level, BSES aggregators need to aggregate the operational feasible regions of all BSES units to form the operational feasible region of the BSES cluster. The aggregated operational feasible region represents the adjustable range of the flexible resources when all BSES units are simultaneously controlled. The mathematical essence of the feasible region aggregation problem is the Minkowski sum (M-Sum). The aggregation calculation process is as follows.

The expression for the aggregated power when the number of BSES units is N is presented in Equation 14.

$$p_{i,t}^{agg} = \sum_{j=1}^{N} p_{j,t}^{ES}, \forall t \in \tau \tag{14}$$

The aggregated feasible domain F can be expressed as Equation 15:

$$F = \bigcup_{j\in\mathcal{N}} F_j \tag{15}$$

where $\cup$ is denoted as Minkowski summation; $\mathcal{N}: = [1, 2, \cdots N]$.

However, when the number of energy storage units in the base station is high, the number of sets and dimensions involved in the operation increases, and the planes describing the boundary of the feasible domain increase exponentially, which leads to the difficulty of the Minkowski summation and makes the solution of its aggregated power feasible domain non-computable. Therefore, in order to reduce the computational complexity, this paper adopts an aggregated power feasible domain maximal inner approximation method (Zhao et al., 2017), whose principle schematic is shown in Figure 2.

The feasible region aggregation problem is characterized by large computational scale and strong temporal coupling. The exact feasible region of the aggregate is often difficult to compute and typically requires approximation of the feasible region for individual objects first. Initially, a basic power feasible region F_0 is selected and subjected to scaling and translation to fit the power feasible regions of each BSES unit. Then, the Minkowski sum is performed. This method effectively addresses the computational complexity of the aggregated feasible region. The fitted power feasible region is represented as Equation 16:

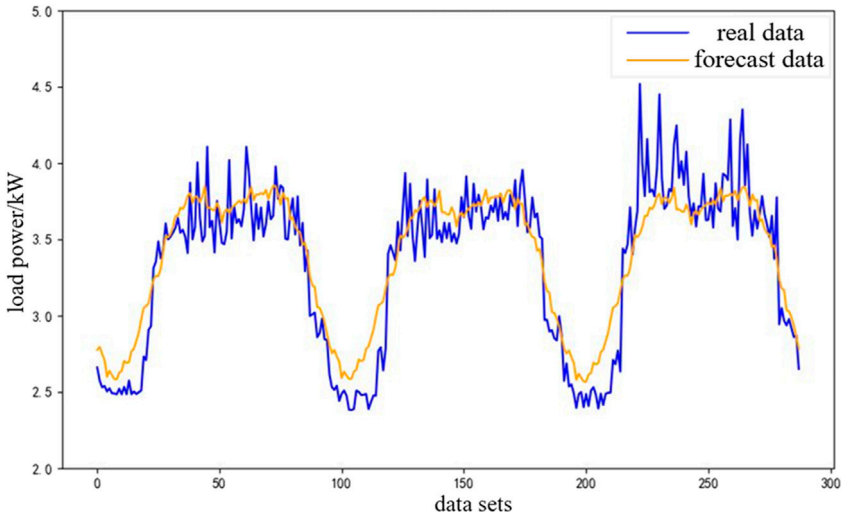

FIGURE 6
5G base station load forecast for three consecutive days.

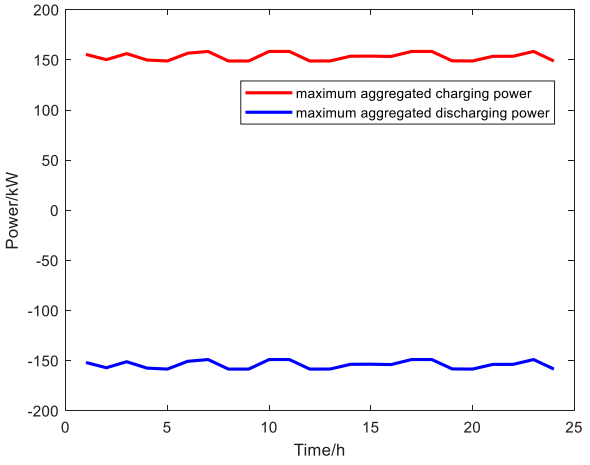

FIGURE 7
Charging and discharging potential of aggregated energy storage for 10 base stations over 24 time periods.

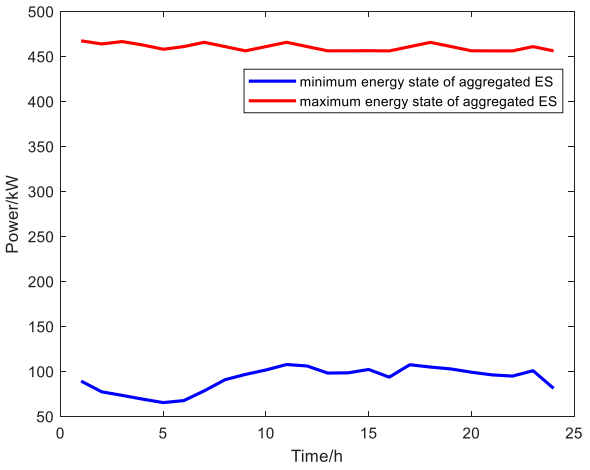

FIGURE 8
Energy state boundaries of aggregated energy storage for 10 base stations over 24 time periods.

$$\varphi_j F_0 + \boldsymbol{\mu}_j = \left\{ y_j \middle| y_j = \varphi_j \xi + \boldsymbol{\mu}_j, \forall \xi \in F_0 \right\} \tag{16}$$

where φ_j is the scaling factor; $\boldsymbol{\mu}_j$ is the translation factor, $\boldsymbol{\mu}_j \in \mathbb{R}^T$, $\mathbb{R}^T$ denotes the T-dimensional real number space; y_j denotes the power feasible domain of the BSES at each moment; ξ denotes the baseline power feasible domain at each moment.

The expression of F_0 is as follows:

$$F_0 = \left\{ \mathbf{p}_0^{ES} \in \mathbb{R}^T \middle| \begin{array}{c} E_{0,t}^{ES} = \hat{\delta} E_{0,t-1}^{ES} + p_{0,t}^{ES} \Delta t, \forall t \in \tau \\ -\hat{P}_{0,t}^{ES,-} \le p_{0,t}^{ES} \le \hat{P}_{0,t}^{ES,+}, \forall t \in \tau \\ \hat{E}_{0,t}^{ES,-} \le E_{0,t}^{ES} \le \hat{E}_{0,t}^{ES,+}, \forall t \in \tau \end{array} \right\} \tag{17}$$

where $\hat{\delta}$, $\hat{p}_{0,t}^{ES,-}$, $\hat{p}_{0,t}^{ES,+}$, $\hat{E}_{0,t}^{ES,-}$, $\hat{E}_{0,t}^{ES,+}$ are the average values of the corresponding parameters for all BSES.

Equation 17 can be written in a compact form, as show in Equation 18:

$$F_0 = \left\{ \mathbf{p}_0^{ES} \in \mathbb{R}^T \middle| \mathbf{M}_0 \mathbf{p}_0^{ES} \le \mathbf{N}_0 \right\} \tag{18}$$

where M_0 and $\mathbf{N}_0$ are expressed as Equations 19, 20, respectively:

$$\mathbf{M}_0 = \left(diag(\mathbf{I}); diag(-\mathbf{I}); \mathbf{A}_0^{-1}\mathbf{B}_0; -\mathbf{A}_0^{-1}\mathbf{B}_0 \right) \tag{19}$$

$$\mathbf{N}_0 = \left(\hat{\mathbf{p}}_0^{ES,+}; \hat{\mathbf{p}}_0^{ES,-}; \hat{\mathbf{E}}_{0,t}^{ES,+} - \mathbf{A}_0^{-1}\mathbf{C}_0; -\hat{\mathbf{E}}_{0,t}^{ES,-} + \mathbf{A}_0^{-1}\mathbf{C}_0 \right) \tag{20}$$

where $\mathbf{B_0} = \mathbf{B_n}$, $\mathbf{A_0}$'s expression is as Equation 21:

$$\mathbf{A_0} = \begin{bmatrix} 1 & 0 & 0 & \cdots & 0 \\ -\hat{\delta} & 1 & 0 & \cdots & 0 \\ 0 & -\hat{\delta} & 1 & \cdots & 0 \\ \vdots & \vdots & \vdots & \ddots & \vdots \\ 0 & 0 & 0 & \cdots & 1 \end{bmatrix} \tag{21}$$

where $\mathbf{A_0} \in \mathbb{R}^{T \times T}$. $\hat{\delta}$ is the average values of self-discharge efficiency of all BSES.

Scaling and translation of F_0 is used to fit each BSES power feasible domain F_n, when φ_j is maximum, the fitted BSES power feasible domain F_j is optimal, and the optimal parameters φ_j^* and $\boldsymbol{\mu}_j^*$ can be obtained by solving the optimization problem as shown in Equation 22:

$$\begin{aligned} &\underset{\varphi_j, \boldsymbol{\mu}_j}{\text{maximize}} \quad \varphi_j \\ &s.t. \quad \varphi_j F_0 + \boldsymbol{\mu}_j \subset F_j \\ &\varphi_j \ge 0 \end{aligned} \tag{22}$$

Let $\phi_j = \frac{1}{\varphi_j}$, $\boldsymbol{\eta}_j = -\phi_j \boldsymbol{\mu}_j$, based on Farkas' theorem, the above optimization problem expression can be transformed into Equation 23:

$$\begin{aligned} &\underset{\phi_j, \boldsymbol{\eta}_j, \mathbf{G}}{\text{minimize}} \quad \phi_j \\ &s.t. \quad \mathbf{G}\mathbf{M_0} = \mathbf{M}_j \\ &\mathbf{G}\mathbf{N_0} \le \phi_j \mathbf{N}_j + \mathbf{M}_j \boldsymbol{\eta}_j \end{aligned} \tag{23}$$

By solving the above optimization problem, the parameters φ_j and $\boldsymbol{\mu}_j$ can be obtained, so that the feasible domain of BSES aggregation power can be obtained as Equation 24:

$$F_{agg} = \left\{ \mathbf{p}_t^{agg} \in \mathbb{R}^T \middle| \begin{array}{c} E_{i,t}^{agg} = \delta_i E_{i,t-1}^{agg} + p_{i,t}^{agg} \Delta t, \forall t \in \tau \\ -p_{i,t}^{agg,-} \le p_{i,t}^{agg} \le p_{i,t}^{agg,+}, \forall t \in \tau \\ E_{i,t}^{agg,-} \le E_{i,t}^{agg} \le E_{i,t}^{agg,+}, \forall t \in \tau \end{array} \right\} \tag{24}$$

where each boundary parameter is expressed as Equations 25-28:

$$\mathbf{p}_i^{agg,-} = \varphi \hat{P}_0^{ES,-} - \boldsymbol{\mu} \tag{25}$$

$$\mathbf{p}_i^{agg,+} = \varphi \hat{P}_0^{ES,+} + \boldsymbol{\mu} \tag{26}$$

$$\mathbf{E}_i^{agg,-} = \varphi \hat{E}_0^{ES,-} - \mathbf{A}^{-1}\mathbf{B}\boldsymbol{\mu} \tag{27}$$

$$\mathbf{E}_i^{agg,+} = \varphi \hat{E}_0^{ES,+} + \mathbf{A}^{-1}\mathbf{B}\boldsymbol{\mu} \tag{28}$$

where $\varphi = \sum_{j \in \Omega_i} \varphi_j^*$, $\boldsymbol{\mu} = \sum_{j \in \Omega_i} \boldsymbol{\mu}_j^*$; Ω_i denotes the set of BSES belonging to aggregator i.

3 5G BSES co-regulation method for voltage regulation in DNs

This chapter aims to study 5G BSES participation in DN coordinated scheduling methods for optimal operation in low-voltage scenarios. It first establishes a DN model and introduces

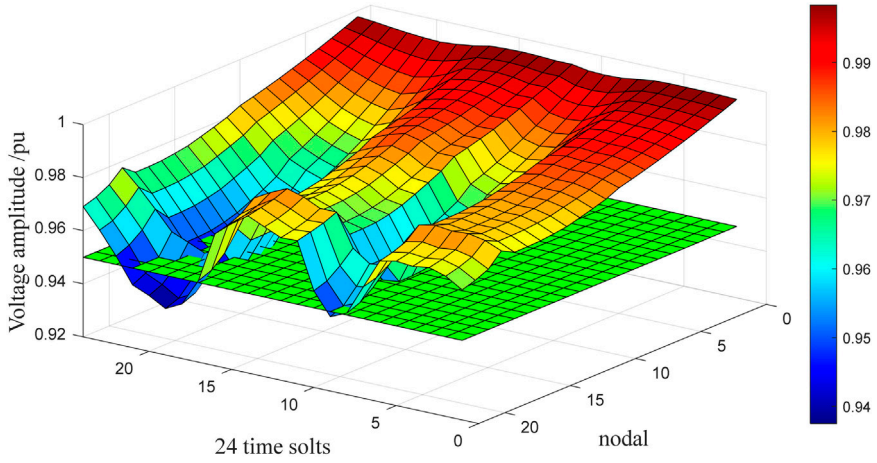

FIGURE 9
Voltage amplitude of BSES before participation in dispatch for 24 time periods.

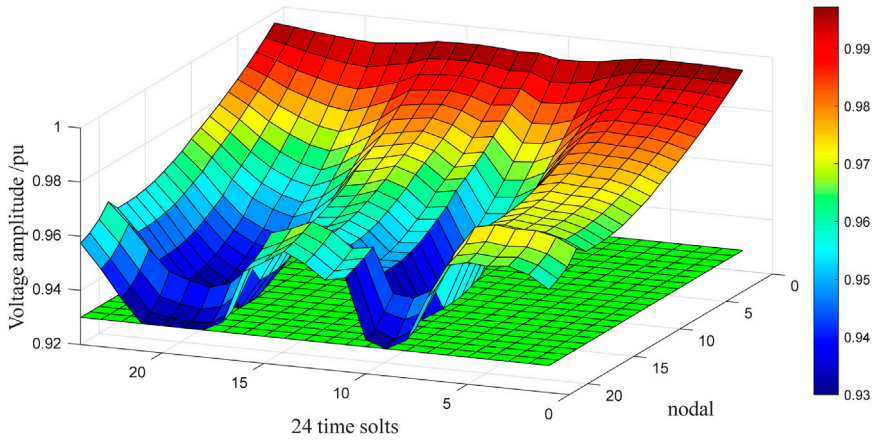

FIGURE 10
Voltage amplitude after participation of BSES in dispatch for 24 time periods.

a quantitative assessment method for low-voltage regulation demand, which guides base station operators in coordinating with the DN. The chapter then proposes a cooperative scheduling method for BSES, optimizing its charging and discharging strategies to regulate DN voltage and improve grid safety and stability.

3.1 DN modeling

3.1.1 DN topology model

Since the DN is a radial structure, the DN topology containing N nodes is defined as $G = (\mathcal{N}, \mathcal{E})$, where $\mathcal{N} = \{1, 2, ..., N\}$ and $\mathcal{E}$ represent the set of nodes and the set of lines, respectively. The substation is denoted as node 0. In addition to the substation, each node i has a unique parent node π_i and a set of child nodes directly connected to it, which are denoted by C_i. Without loss of generality, the node index is encoded in such a way that the index of each node is always greater than the index of its parent node, $\pi_i < i$. In addition, the line pointing from a node π_i to node i is labeled as line i. Therefore, the branch numbering $\mathcal{E} = \{1, 2, ..., N\}$ can be consistent with the node numbering. Let A^0 be an $N \times (N + 1)$ dimensional node association matrix. It can be expressed as Equation 29:

$$A_{ij}^0 = \begin{cases} -1 & j = i \\ 1 & j = \pi_i \\ 0 & j \neq i, \pi_i \end{cases} \tag{29}$$

where if $j = \pi_i$, $A_{ij}^0 = 1$ indicates that node j is the parent of node i and there is a line connecting node i to node j. If $A_{ij}^0 = 0$, it indicates that node j is not the parent of node i. A^0 is divided into two parts, a and A, where a represents the first column of A^0, which is the correlation matrix of node 0. A is a full-rank matrix, and therefore A is invertible.

3.1.2 DN branch-circuit current modeling

For a radial DN, the following tidal equations are used to represent the branch-circuit tidal models (Li et al., 2019).

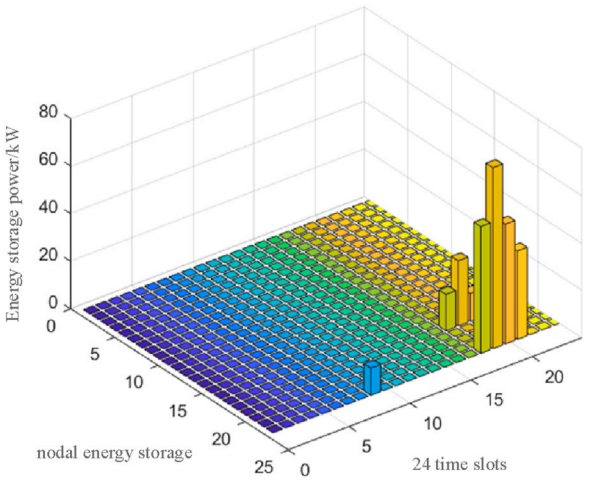

FIGURE 11
24 time periods of AES regulation requirements at each node.

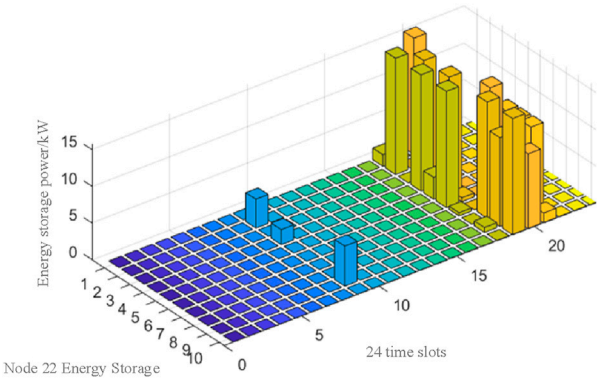

FIGURE 12
Charging and discharging of internal BSES at node 22 for 24 time periods.

$$P_i - \frac{P_i^2 + Q_i^2}{V_{\pi_i}^2} r_i + p_i = \sum_{j \in C_i} P_j \quad \forall i \in \mathcal{N}/0 \tag{30}$$

$$Q_i - \frac{P_i^2 + Q_i^2}{V_{\pi_i}^2} x_i + q_i = \sum_{j \in C_i} Q_j \quad \forall i \in \mathcal{N}/0 \tag{31}$$

$$V_{\pi_i}^2 - V_i^2 = 2\left(r_i P_i + x_i Q_i\right) - \left(r_i^2 + x_i^2\right) \frac{P_i^2 + Q_i^2}{V_{\pi_i}^2} \quad \forall i \in \varepsilon \tag{32}$$

Equations 30, 31 represent the active and reactive power balance at node i, respectively, and Equation 32 represents the voltage link between two neighboring nodes, Where p_i and q_i denote the active and reactive power injected at node i, respectively; P_i and Q_i denote the active and reactive power circulating on branch i, respectively; r_i and x_i denote the resistance and reactance of line i, respectively; and V_{π_i} and V_i denote the voltage magnitude of the parent node and the child node i, respectively.

Since the original branch-current models (30)–(32) are non-convex, the convex optimization solution method cannot be directly applied. To ensure the efficient solution of the problem, after approximating, and neglecting the higher terms of the equations, the linear branch-current model can be obtained as shown in Equations 33–35.

$$P_i - \sum_{j \in C_i} P_j = -p_i \quad \forall i \in \mathcal{N}/0 \tag{33}$$

$$Q_i - \sum_{j \in C_i} Q_j = -q_i \quad \forall i \in \mathcal{N}/0 \tag{34}$$

$$V_{\pi_i} - V_i = r_i P_i + x_i Q_i \quad \forall i \in \varepsilon \tag{35}$$

3.2 BSES demand assessment model for voltage regulation in DNs

3.2.1 Objective function

When the distribution network system experiences excessive load, certain nodes may encounter low voltage issues. These issues can be addressed by aggregators scheduling the charging and discharging actions of 5G BSES, effectively adjusting the flexible active load of the 5G base stations. From the perspective of the power grid, the aim is to resolve low voltage problems with minimal energy storage adjustment requirements. Therefore, the objective function is to minimize the energy storage adjustment demand F at each node of the base station over a day, as shown in Equation 36.

$$F = \sum_{t=1}^{T=24} \sum_{i=1}^{N_e} \left| p_{i,t}^{agg} \right| \tag{36}$$

where T is 24 time periods in a day; N_e denotes the number of node's aggregated energy storage (AES); $p_{i,t}^{agg}$ denotes the output power of node i's AES in time period t.

3.2.2 Restrictive condition

3.2.2.1 Linear branch flow model

$$P_{i,t} - \sum_{j \in C_i} P_{j,t} = -p_{i,t} \quad \forall i \in \mathcal{N}/0 \tag{37}$$

$$Q_{i,t} - \sum_{j \in C_i} Q_{j,t} = -q_{i,t} \quad \forall i \in \mathcal{N}/0 \tag{38}$$

$$V_{\pi_i,t} - V_{i,t} = r_i P_{i,t} + x_i Q_{i,t} \quad \forall i \in \varepsilon \tag{39}$$

Equations 37-39 represent the linear power flow constraints of the line where $p_{i,t}$ and $q_{i,t}$ denote the active and reactive power injected into node i at time t; $P_{i,t}$ and $Q_{i,t}$ denote the active and reactive power circulating on branch i at time t; r_i and x_i denote the resistance and reactance of line i; $V_{\pi_i,t}$ and $V_{i,t}$ denote the voltage magnitude of the parent node and the child node i at time t, respectively.

3.2.2.2 Nodal power balance constraints

$$p_{i,t} = -p_{i,t}^d - p_{i,t}^{agg} \tag{40}$$

$$q_{i,t} = -q_{i,t}^d \tag{41}$$

Equation 40 ensures the load active power balance of node i; Equation 41 ensures the load reactive power balance of node I, where $p_{i,t}^d$ and $q_{i,t}^d$ denote the load active power and reactive power of node i at time t respectively; $p_{i,t}^{agg}$ denote the AES output power of node i at time t.

3.2.2.3 Node voltage constraints

$$\underline{V}_i \le V_{i,t} \le \bar{V}_i \tag{42}$$

Equation 42 ensures that the node voltage of the DN does not exceed the limit. Where $\underline{V}_i$ and $\bar{V}_i$ are the maximum and minimum values allowed for the nodal voltage, respectively.

3.2.2.4 Line transmission power capacity constraints

$$P_{i,t}^2 + Q_{i,t}^2 \le S_{i,t}^2 \tag{43}$$

where $S_{i,t}$ is denoted as the maximum value of the apparent power allowed to flow through branch *i*. In order to facilitate the solution, it is necessary to linearize the line transmission power capacity constraint, as shown in Equation 44. Equation 44 ensures that the transmission power of the DN line does not exceed the limit.

$$\begin{cases} (\sqrt{2}-1)P_{i,t} + Q_{i,t} \le S_{i,t} \\ \sqrt{2}\,P_{i,t} - (\sqrt{2}-2)Q_{i,t} \le \sqrt{2}\,S_{i,t} \\ \sqrt{2}\,P_{i,t} + (\sqrt{2}-2)Q_{i,t} \le \sqrt{2}\,S_{i,t} \\ (\sqrt{2}-1)P_{i,t} - Q_{i,t} \le S_{i,t} \\ -(\sqrt{2}-1)P_{i,t} + Q_{i,t} \le S_{i,t} \\ -\sqrt{2}\,P_{i,t} - (\sqrt{2}-2)Q_{i,t} \le \sqrt{2}\,S_{i,t} \\ -\sqrt{2}\,P_{i,t} + (\sqrt{2}-2)Q_{i,t} \le \sqrt{2}\,S_{i,t} \\ -(\sqrt{2}-1)P_{i,t} - Q_{i,t} \le S_{i,t} \end{cases} \tag{44}$$

3.2.2.5 The power and energy state constraints of the AES

$$E_{i,t}^{agg} = \delta_i E_{i,t-1}^{agg} + p_{i,t}^{agg}\Delta t \tag{45}$$

$$-p_{i,t}^{agg,-} \le p_{i,t}^{agg} \le p_{i,t}^{agg,+} \tag{46}$$

$$E_{i,t}^{agg,-} \le E_{i,t}^{agg} \le E_{i,t}^{agg,+} \tag{47}$$

Equations 45-47 indicates the operational constraints of AES where $E_{i,t}^{agg}$ denotes the residual energy state of the AES *i* at time *t*; δ_i denotes the self-discharge efficiency of the AES *i*; Δt denotes the charging or discharging time period of the AES; $p_{i,t}^{agg,+}$ denotes the maximum charging power of the AES; $p_{i,t}^{agg,-}$ denotes the maximum discharging power of the AES; $E_{i,t}^{agg,+}$ denotes the maximum permissible energy state value of the AES *i* at time *t*; $E_{i,t}^{agg,-}$ denotes the minimum permissible energy value of the AES *i* at time *t*.

3.3 Cooperative scheduling model of BSES for voltage regulation in DNs

Building on the BSES demand assessment model for low voltage regulation in distribution networks, the power adjustment demand for aggregated BSES at each network node has been calculated. However, the individual BSES output at each node remains unknown. To address this, an optimized scheduling model is proposed, which balances the state of charge and optimizes BSES charging and discharging strategies to mitigate low voltage issues in the distribution network.

3.3.1 Objective function

Charging and discharging is carried out with the goal that the SOC of each base station's energy storage state of charge is close to 0.5 after scheduling, to realize the fair distribution of power among each base station's energy storage resources, as shown in Equation 48.

$$F = \sum_{j=1}^{N}\sum_{t=1}^{T}\left|SOC_{j,t}^{ES} - 0.5\right| \tag{48}$$

where N denotes the number of BSES inside the node; T denotes the BSES scheduling time period; $SOC_{j,t}^{ES} = \frac{E_{j,t}^{ES}}{E_j^B}$ denotes the SOC state of BSES *j* inside the node at time *t*, $E_{j,t}^{ES}$ denotes the remaining energy state of BSES *j* inside the node at time *t*, and E_j^B denotes the rated capacity of BSES *j* inside the node.

3.3.2 Restrictive condition

3.3.2.1 Energy storage energy balance constraints

The sum of the node's internal BSES energy should be balanced with the node's AES energy value, as described in Equation 49.

$$\sum_{j=1}^{N} E_{j,t}^{ES} = E_{i,t}^{agg} \tag{49}$$

3.3.2.2 Energy storage energy state constraints

$$E_{j,t}^{ES} = \delta_j \cdot E_{j,t-1}^{ES} + p_{j,t}^{ES}\Delta t \tag{50}$$

$$E_{j,t}^{ES,-} \le E_{j,t}^{ES} \le E_{j,t}^{ES,+} \tag{51}$$

Equation 50 illustrates the relationship between the energy stored in BSES *j* and its input power, Equation 51 shows the upper and lower bounds of energy stored in BSES *j* where δ_j denotes the self-discharge efficiency of the BSES *j*; $p_{j,t}^{ES}$ denotes the output power of the BSES *j* at time *t*; Δt denotes the BSES charging or discharging time period; $E_{j,t}^{ES,-}$ denotes the minimum energy state value allowed by the BSES *j* at time *t*; and $E_{j,t}^{ES,+}$ denotes the maximum energy state value allowed by the BSES *j* at time *t*.

3.3.2.3 Energy storage power balance constraints

$$\sum_{j=1}^{N} p_{j,t}^{ES} = p_{i,t}^{agg} \tag{52}$$

$$-p_{j,t}^{ES,-} \le p_{j,t}^{ES} \le p_{j,t}^{ES,+} \tag{53}$$

Equation 52 ensures the power balance of AES, Equation 53 enforces the lower and upper bounds to the power input of BSES *j* where $p_{j,t}^{ES,+}$ indicates the maximum charging power of the BSES; $p_{j,t}^{ES,-}$ indicates the maximum discharging power of the BSES *j*.

4 Simulation results

4.1 System data

To validate the effectiveness of the proposed method, a simulation analysis was conducted using a 22-node distribution network in a specific region. The network topology is shown in Figure 3, and the line parameters are listed in Table 1. The nodes are uniformly distributed, with the maximum and minimum node voltages set at 1.05 p. u and 0.95 p. u, respectively. The typical

daily load curve is depicted in Figure 4. In this region, the communication base stations are equipped with energy storage systems with a rated capacity of 48 kWh and a maximum charge/discharge power of 15.84 kW. The self-discharge efficiency is set at 0.99, and the state of charge (SOC) is allowed to range between a maximum of 0.9 and a minimum of 0.1.

4.2 5G BSES energy consumption prediction model results and analysis based on LSTM

The training and test datasets were imported into the LSTM-based load forecasting model for 5G base stations. The error convergence for the training and test datasets is shown in Figure 5, while the load forecasting for the test dataset samples is illustrated in Figure 6. The root mean square error (RMSE) for the test dataset samples was calculated to be 0.22 kW, with an average relative error of 0.06. As seen in Figure 5, the loss function value converges to a minimum after 24 training epochs. Figure 6 indicates that the model accurately reflects the load data trends over time, demonstrating good tracking performance. In summary, these results validate that the LSTM load forecasting model performs well in predicting the load data of 5G base stations.

4.3 Results and analysis of BSES aggregation

The simulation results for the aggregated power feasible region of 10 BSES units are shown below. Figures 7, 8 illustrate the charging and discharging potential and the energy state boundaries of the aggregated 10 base stations over 24 time periods in a day. The adjustable capacity of the aggregated energy storage is influenced by factors such as individual BSES parameters and the load size of the base stations, resulting in temporal fluctuations. The charging and discharging potential is related to the charge/discharge power parameters of each storage unit. The minimum energy state of the aggregated storage is associated with the base station load size, while the maximum energy state is linked to the rated capacity parameters of each storage unit. Therefore, the proposed BSES aggregation model can quantitatively assess the charging and discharging potential and the adjustable capacity of the controllable BSES group, providing data support for the subsequent participation of BSES in coordinated scheduling with the distribution network.

4.4 Validation results of 5G BSES co-regulation method for DN voltage regulation

4.4.1 Validation results of a BSES demand assessment model for DN voltage regulation

Based on the distribution network branch power flow model presented in this paper and utilizing existing data, the voltage magnitudes at each node of the distribution network were calculated before the participation of BSES in the scheduling across multiple time scales. Figure 9 illustrates the voltage magnitudes at each node of the distribution network over 24 time periods before BSES participated in the scheduling. As shown in the figure, low voltage phenomena (voltage magnitude per unit value less than 0.95, indicated by the green sections) occur at certain times at the end nodes of the distribution network.

Using the BSES demand assessment model proposed in this paper, and combining it with existing data, the voltage magnitudes at each node of the distribution network and the energy storage adjustment requirements for low voltage mitigation were calculated after the participation of BSES in the scheduling across multiple time scales. Figure 10 shows the voltage magnitudes at each node of the distribution network over 24 time periods after the BSES participated in the scheduling. As depicted in the figure, the coordinated scheduling of BSES effectively improves the voltage magnitudes at the end nodes, achieving low voltage mitigation. The multi-time scale adjustment requirements of the aggregated BSES power for low voltage mitigation in the distribution network nodes are shown in Figure 11.

4.4.2 Validation results of an optimal scheduling model for BSES for voltage regulation in DNs

Based on the BSES optimization scheduling model proposed in this paper and utilizing existing data, the coordinated scheduling of BSES at each node was calculated. Taking node 22 as an example for the analysis of internal BSES coordination, Figure 12 illustrates the charging and discharging conditions of BSES at node 22 over 24 time periods. The figure shows that the model can achieve coordinated scheduling of BSES, optimizing the charging and discharging strategies of the energy storage units and effectively managing low voltage issues.

5 Conclusion

In this paper, a BSES aggregation method that takes into account both the base station energy consumption and the backup power characteristics of BSES is proposed. Furthermore, with the goal of fully utilizing the energy storage resources of 5G base stations, a BSES co-regulation method for voltage regulation in DNs is proposed. The feasibility of the proposed method is verified by case analysis, and the following conclusions can be drawn.

- The 5G base station energy consumption prediction model based on LSTM proposed in this paper takes into account the energy consumption characteristics of 5G base stations. The prediction results have high accuracy and provide data support for the subsequent research on BSES aggregation and optimal scheduling.
- The BSES aggregation model proposed in this paper, which considers the prediction of base station energy consumption, accurately and quantitatively evaluates the power adjustability and adjustable capacity of BSES clusters, and enables the centralized management and scheduling of massive BSES.
- The BSES optimization scheduling model constructed in this paper for voltage regulation of DNs further exploits the dispatchable potential of BSES to participate in DN synergy and interaction. It addresses the low-voltage problem of the

DN and improves the security and stability of the grid while ensuring a sufficient and stable backup supply for 5G base stations.

Data availability statement

The original contributions presented in the study are included in the article/supplementary material, further inquiries can be directed to the corresponding author.

Author contributions

PS: Conceptualization, Data curation, Formal Analysis, Methodology, Validation, Writing–original draft. MZ: Supervision, Validation, Writing–review and editing. HL: Investigation, Methodology, Writing–original draft. YD: Investigation, Methodology, Writing–original draft. QR: Investigation, Methodology, Writing–original draft.

Funding

The author(s) declare that no financial support was received for the research, authorship, and/or publication of this article.

Conflict of interest

The authors declare that the research was conducted in the absence of any commercial or financial relationships that could be construed as a potential conflict of interest.

Publisher's note

All claims expressed in this article are solely those of the authors and do not necessarily represent those of their affiliated organizations, or those of the publisher, the editors and the reviewers. Any product that may be evaluated in this article, or claim that may be made by its manufacturer, is not guaranteed or endorsed by the publisher.

References

Althoff, M., Stursberg, O., and Buss, M. (2010). Computing reachable sets of hybrid systems using a combination of zonotopes and polytopes. *Nonlinear Anal. Hybrid. Syst.* 4 (2), 233–249. doi:10.1016/j.nahs.2009.03.009

Barot, S., and Taylor, J. A. (2017). A concise, approximate representation of a collection of loads described by polytopes. *Int. J. Electr. Power & Energy Syst.* 84, 55–63. doi:10.1016/j.ijepes.2016.05.001

Chai, B., Chen, J., Yang, Z., and Zhang, Y. (2014). Demand response management with multiple utility companies: a two-level game approach. *IEEE Trans. Smart Grid* 5 (2), 722–731. doi:10.1109/tsg.2013.2295024

Cheng, J., Zhang, H., and Xu, J. (2023) "Traffic prediction model for telecommunication base stations based on improved WOA optimized LSTM and EMD," in *2023 IEEE 5th international conference on power, intelligent computing and systems (ICPICS)*, 1075–1084.

Fu, L. (2020) "Time series-oriented load prediction using deep peephole LSTM," in *2020 12th international conference on advanced computational intelligence (ICACI)*, 86–91.

Han, J., Liu, N., Huang, Y., and Zhou, Z. (2021). Collaborative optimization of distribution network and 5G mobile network with renewable energy sources in smart grid. *Int. J. Electr. Power & Energy Syst.* 130, 107027. doi:10.1016/j.ijepes.2021.107027

Jia, Z., Gao, H., Yang, Y., Liu, L., Li, Z., Liu, S., et al. (2023) "Research on mobile energy storage technology based on improving distributed energy consumption in substation area," in *2023 IEEE 7th information technology and mechatronics engineering conference (ITOEC)*, 156–159.

Li, C., Wang, Y., Wang, R., Liu, H., Tao, X., Zhong, H., et al. (2022) "Load recovery strategy based on mobile energy storage flexibility and DN reconfiguration," in *2022 IEEE 5th international electrical and energy conference (CIEEC)*, 2905–2910.

Li, J., Xu, Z., Zhao, J., and Zhang, C. (2019). Distributed online voltage control in active distribution networks considering PV curtailment. *IEEE Trans. Industrial Inf.* 15 (10), 5519–5530. doi:10.1109/tii.2019.2903888

Liang, H., Li, J., Deng, Y., Song, F., and Yu, X. (2023) "Optimization method for energy storage system planning based on dispatchable potential of 5G base station and cluster partition of DN," in *2023 IEEE 6th international electrical and energy conference (CIEEC)*, 4334–4340.

Ma, J., Silva, V., Belhomme, R., Kirschen, D. S., and Ochoa, L. F. (2013). Evaluating and planning flexibility in sustainable power systems. *IEEE Trans. Sustain. Energy* 4 (1), 200–209. doi:10.1109/tste.2012.2212471

Morosi, S., Piunti, P., and Del Re, E. (2013) "A forecasting driven technique enabling power saving in LTE cellular networks," in *2013 IEEE 9th international conference on wireless and mobile computing, networking and communications (WiMob)*, 217–222.

Müller, F. L., Szabó, J., Sundström, O., and Lygeros, J. (2019). Aggregation and disaggregation of energetic flexibility from distributed energy resources. *IEEE Trans. Smart Grid* 10 (2), 1205–1214. doi:10.1109/tsg.2017.2761439

Pan, H., Liu, J., Zhou, S., and Niu, Z. (2015). A block regression model for short-term mobile traffic forecasting. *IEEE/CIC Int. Conf. Commun. China (ICCC)*, 1–5. doi:10.1109/iccchina.2015.7448619

Qu, H., Ma, W., Zhao, J., and Wang, T. (2013). Prediction method for network traffic based on Maximum Correntropy Criterion. *China Commun.* 10 (1), 134–145. doi:10.1109/cc.2013.6457536

Qu, H., Zhang, Y., and Zhao, J. (2019) "A spatio-temporal traffic forecasting model for base station in cellular network," in *2019 IEEE 19th international conference on communication technology (ICCT)*, 567–571.

Sajjad, I. A., Chicco, G., and Napoli, R. (2016). Definitions of demand flexibility for aggregate residential loads. *IEEE Trans. Smart Grid* 7 (6), 2633–2643. doi:10.1109/tsg.2016.2522961

Shang, Y., Liu, J., Ma, J., Qiu, Y., Zhang, Z., and Liu, C. (2022) "A prediction method of 5G base station cell traffic based on improved transformer model," in *2022 IEEE 4th international conference on civil aviation safety and information technology (ICCASIT)*, 40–45.

Stolojescu-Crisan, C. (2012) "Data mining based wireless network traffic forecasting," in *2012 10th international symposium on electronics and telecommunications*, 115–118.

Suo, S., Kuang, X., Cheng, R., Chen, L., Huang, K., and Zhao, W. (2022) "Research of real-time monitoring and control technology for distributed energy storage based on 5G," in *2022 IEEE/IAS industrial and commercial power system asia (I&CPS asia)*, 1496–1500.

Yang, J., Lin, G., Lv, R., Gao, C., and Chen, T. (2020) "Research on construction and dispatching of virtual power plant based on reserve energy storage of communication base station," in *2020 IEEE 4th conference on energy internet and energy system integration (EI2)*, 398–403.

Yang, L., Zhang, L., Yu, K., and Ma, X. (2023) "Research on interaction between power grid and 5G communication base station storage energy," in *2023 8th asia conference on power and electrical engineering*. IEEE: ACPEE, 592–596.

Ye, G. (2021) "Research on reducing energy consumption cost of 5G Base Station based on photovoltaic energy storage system," in *2021 IEEE international conference on computer science, electronic information engineering and intelligent control technology (CEI)*, 480–484.

Yin, X., Lv, G., Wang, Z., Lu, Z., Liu, Y., and Yu, K. (2022) "Research on 5G BSES configuration taking photovoltaics into account," in *2022 7th asia conference on power and electrical engineering (ACPEE)*, 591–595.

Yu, K., Yang, L., Zhang, L., and Ma, X. (2023) "Summary of research on key technologies of 5G base station flexible resources," in *2023 8th asia conference on power and electrical engineering*. IEEE: ACPEE, 2129–2133.

Zhang, L., Yu, K., Yang, L., and Ma, X. (2023) "A study on energy storage configuration of 5G communication base station participating in grid interaction," in *2023 8th asia conference on power and electrical engineering*. IEEE: ACPEE, 608–612.

Zhao, L., Zhang, W., Hao, H., and Kalsi, K. (2017). A geometric approach to aggregate flexibility modeling of thermostatically controlled loads. *IEEE Trans. Power Syst.* 32 (6), 4721–4731. doi:10.1109/tpwrs.2017.2674699

Zhou, Q., and Xu, Y. (2021) "Reactive power optimization of active DN considering mobile energy storage," in *2021 international conference on power system technology (POWERCON)*, 1040–1044.